Characterization of PtSn nanoparticles in KL zeolite and *n*-hexane aromatization activity

Sung June Cho[a,*], and Ryong Ryoo[b]

[a]*National Research Laboratory for Clean Energy Technology, Department of Applied Chemical Engineering and the Research Institute for Catalysis, Chonnam National University, Yong Bong 300, Buk-gu, Gwang-ju 500-757, Korea*

[b]*Department of Chemistry, Korea Advanced Institute of Science and Technology, Taeduk Science Town, Taejon, 305-701 Korea*

Received 27 February 2004; accepted 27 May 2004

Bimetallic nanoparticles of Pt and Sn have been prepared with an ion exchange of Sn^{2+} ions into KL zeolite containing 1-nm Pt nanoparticles. Incorporation of Sn does not cause a blockage for xenon adsorption. The results of data analysis of X-ray absorption fine structure show that the obtained particle size does not increase significantly. The microstructure of the PtSn nanoparticles seems to be Pt core covered with Sn. The obtained PtSn nanoparticles show a high selectivity to benzene with a comparable turnover rate for *n*-hexane aromatization.

KEY WORDS: PtSn nanoparticles; KL zeolite; *n*-hexane aromatization.

1. Introduction

PtSn bimetallic nanoparticles have drawn much attention due to a high resistance to coke deposition during naphtha reforming [1,2]. Incorporation of tin into Pt nanoparticles and bulk Pt surface is known to lead to a formation of PtSn nanoparticles and Sn/Pt surface alloy, respectively. Meriaudeau *et al.* [3] prepared the PtSn nanoparticles on NaY zeolite by contacting Pt surface covered with hydrogen with tetramethyltin compound, thereby reacting the alkyltin compound with Pt surface. For Sn/Pt(111) surface alloy, Xu *et al.* [4] found the substantial electronic effect by tin incorporation on adsorption–desorption kinetics of cyclohexane and benzene. It was noteworthy that tin converts most of the strongly chemisorbed benzene to physisorbed one. Cortright and Dumesic [5] obtained PtSn nanoparticles inside KL zeolite channel by reduction with H_2 at 773 K after the impregnation of tributyltin acetate onto the zeolite followed by a second impregnation of $Pt(NH_3)_4(NO_3)_2$. The catalysts showed a high activity and selectivity of isobutane dehydrogenation, which was attributed to the reduced Pt ensemble size by tin and potassium, and zeolite pore structure.

In the previous report, it was shown that Pt nanoparticles consisting of 5–7 atoms can be obtained inside KL zeolite channel with a calcination by O_2 at 593 K and subsequent reduction in H_2 at 573 K after ion exchange of $Pt(NH_3)_4^{2+}$ into the KL zeolite [6]. In this work, we have investigated the formation of PtSn bimetallic nanoparticles on the KL zeolite using a sequential loading method. The obtained PtSn/KL catalyst has been characterized with hydrogen chemisorption, ^{129}Xe NMR spectroscopy, xenon adsorption, X-ray absorption fine structure (XAFS). *n*-Hexane aromatization has been performed over the PtSn/KL catalyst in order to investigate the effect of the formation of bimetallic nanoparticles.

*To whom correspondence should be addressed.

2. Experimental

2.1. Preparation of SnPt nanoparticles supported on KL zeolite (SnPt/KL)

A single batch of 2 wt% Pt/KL, ~5 g was prepared following the procedure described earlier in our previous work [6]. Briefly, 2 wt% Pt/KL was obtained from the activation in O_2 at 593 K for 2 h and the subsequent reduction with H_2 at 573 K for 2 h after the ion exchange of $Pt(NH_3)_4^{2+}$ ($Pt(NH_3)_4(NO_3)_2$, Aldrich) into KL zeolite (ELZ-L, Union Carbide, $K_9[(AlO_2)_9(SiO_2)_{27}]$), similar to the preparation method of Pt/NaY [7] and Pt/EMT [8]. The platinum reduction was followed by the evacuation under nominal pressure of 1×10^{-3} Pa, while the temperature was increased linearly to 673 K for 1 h and maintained at 673 K for 2h, to remove chemisorbed hydrogen. The obtained KL zeolite containing Pt has a molar composition of $Pt_{0.26}$-$K_{8.49}H_{0.51}[(AlO_2)_9(SiO_2)_{27}]$ after all pretreatments.

Sn^{2+} ($SnCl_2$, >99%, Junsei) was exchanged at room temperature for overnight onto the 2.0 wt% Pt/KL sample at pH 3.6, in order to avoid a formation of SnO and SnO_2 precipitates. The ion exchanged zeolites were filtered, washed with doubly distilled water, dried in a vacuum oven at room temperature, and subsequently placed on a fritted disk inside a Pyrex U-tube flow reactor. The zeolite was reduced with heating in H_2 flow (99.999%, passed through a MnO/SiO_2 trap). The H_2

1011-372X/04/0800–0071/0 © 2004 Plenum Publishing Corporation

flow rate for the reduction was 200 mL min^{-1} g^{-1}, and the reduction temperature was linearly increased from room temperature to 573 K over 4 h and maintained at 573 K for 2 h. The Sn/Pt ratio was controlled to 0.1, 0.2 and 0.4, respectively where the content of potassium can be varied from 8.49 K^+ to 8.29 K^+ per unit cell when all the ion-exchanged tin replaced potassium ions.

2.2. Characterization of the SnPt/KL catalyst

Xenon and hydrogen adsorption measurements were performed at 296 K with a conventional volumetric gas adsorption apparatus following the method described in the literature [6,7]. ^{129}Xe NMR spectra were obtained from the adsorbed gas at 296 K with a Bruker AM 300 instrument operating at 83.0 MHz for ^{129}Xe with a 0.5-s relaxation delay. The chemical shift is referenced to xenon gas extrapolated to zero pressure.

X-ray absorption fine structure (XAFS) in He gas was measured at the Pt L_{III} edge at room temperature using Beam Line 10B at the Photon Factory in Tsukuba. The details of the cell preparation and the measurement condition can be found elsewhere [6].

2.3. Catalytic activity measurement of n-hexane aromatization

The rate of catalytic aromatization of *n*-hexane was measured with typically 50 mg catalyst using a Pyrex batch recirculation rig similar to the one described by Schlatter and Boudart [9]. The reactant gas consisted of *n*-hexane, H_2 and He with partial pressure 6, 36 and 59 kPa, respectively. *n*-Hexane (Merck, HPLC grade) was used after purification through three freeze-evacuation-thaw cycles. The total volume of the rig was 620 mL. The gas recirculation rate was 4.0 L min^{-1}. The reaction temperature was controlled to 671 ± 1 K. Products were analyzed with a gas chromatograph (HP5890 Series II) equipped with Carbowax 20 M column using a flame ionization detector.

3. Results and discussion

The previous studies on Pt/KL catalyst showed that Pt nanoparticles containing 5–7 atoms on the average can be prepared independent of Pt content up to 5.2 wt% without a pore blockage for xenon adsorption [6]. Figure 1 shows xenon adsorption isotherms on the PtSn/KL catalysts at 296 K. Amount of xenon adsorption per unit cell for the PtSn/KL catalysts was the same as that of KL zeolite, indicating no pore blockage for xenon adsorption upon the incorporation of tin. The incorporation of tin into the Pt/KL catalyst seems not to cause the growth of particle size in the PtSn/KL catalyst.

Results of hydrogen adsorption on the PtSn/KL catalysts are presented in Table 1. The amount of total hydrogen adsorption on the PtSn/KL catalysts decreased too much, compared to that of the Pt/KL catalyst. Further, all the adsorption became reversible. Therefore, tin seems to cover the hydrogen adsorption site of Pt nanoparticle blocking a strong adsorption of hydrogen. The complete removal of adsorbed hydrogen at room temperature made it difficult to measure the amount of xenon adsorption only on Pt nanoparticles that can be obtained from the difference between two xenon adsorption isotherms before and after hydrogen chemisorption. It was believed that unique gas adsorption characteristics come from the interaction Sn and Pt nanoparticles.

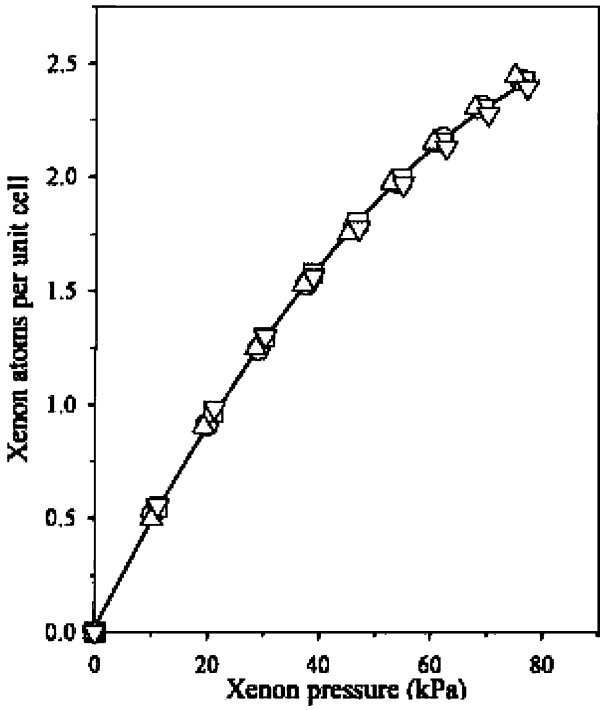

Figure 1. Xenon adsorption isotherms of the PtSn/KL catalysts with an atomic ratio of 0.0 (O), 0.1 (□), 0.2 (Δ) and 0.4 (∇) obtained at 296 K.

Table 1
Hydrogen chemisorption and xenon adsorption on the PtSn/KL catalysts

Sn/Pt	H_{total}/Pt_{total} [a]	H_{rev}/Pt_{rev} [b]	Xe/Pt_{total} [c]
0.0	1.6	0.5	0.20
0.1	1.0	1.0	~0
0.2	0.6	0.6	~0
0.4	0.6	0.6	~0

[a]Total hydrogen chemisorption at 296 K, based on the total amount of Pt.
[b]Reversible hydrogen chemisorption at 296 K, based on the total amount of Pt.
[c]Xenon adsorption on the PtSn nanoparticles at the saturation obtained from the difference between two xenon adsorption isotherms with and without chemisorbed hydrogen based on the total amount of Pt.

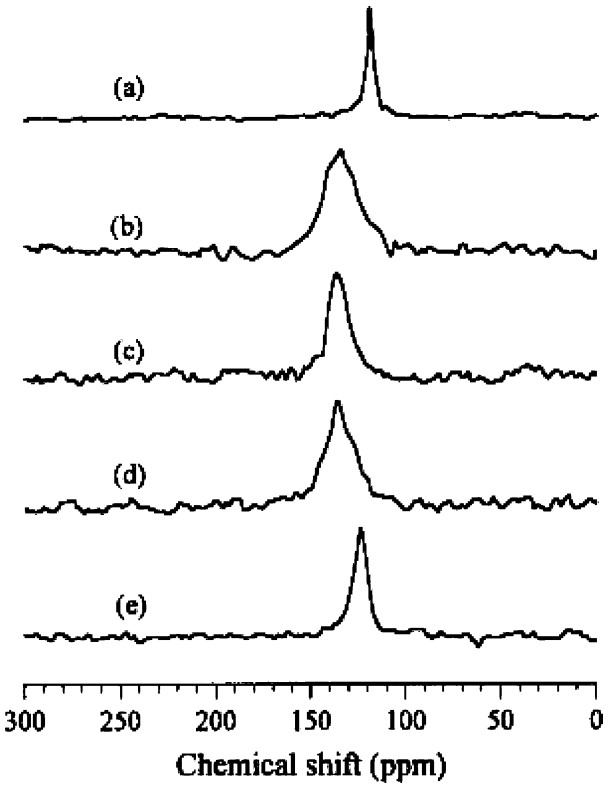

Figure 2. ^{129}Xe NMR spectra of xenon adsorbed on the PtSn/KL catalysts at 296 K and under 53.3 kPa: (a) KL zeolite; (b) 2 wt% Pt/KL; the PtSn/KL with an atomic ratio of (c) 0.1, (d) 0.2 and (e) 0.4.

^{129}Xe NMR spectra of xenon adsorbed on the PtSn/KL catalysts are shown in figure 2. The chemical shift of xenon adsorbed on the PtSn nanoparticles decreased from 137 ppm to 123 ppm upon tin incorporation. The chemical shift of the PtSn/KL catalyst with an atomic ratio of 0.4 was similar to that of the Pt/KL catalyst with chemisorbed hydrogen. According to the previous reports, the interaction of xenon with the Pt nanoparticles can be inhibited due to the increase of surface coverage by metals such as Ag [10] and Cu [11], since these metals have no interaction with xenon. Thus, the decrease of the chemical shift for the PtSn/KL catalyst was consistent with the coverage of Sn on Pt nanoparticles if Sn plays a same role as Ag and Cu.

XAFS spectra for the PtSn/KL catalysts were obtained above the Pt L_{III} edge and analyzed with the UWXAFS2 and FEFF5 [12–14]. The best curve fits are shown as dotted curves in figure 3. The structural parameters obtained through the curve fitting are listed in Table 2. The Pt–Pt coordination number (CN) in the PtSn/KL catalysts did not change significantly upon the incorporation of tin. This result of CN meant that there was no increase of the particle size. The Pt–Pt distance increased to 0.272 nm from 0.258 nm for the PtSn/KL catalysts like a structural relaxation by hydrogen adsorption on Pt nanoparticles. The coordination number of the Pt–Sn pair did not increase with the Sn/Pt ratio since the structural relaxation occurred and there

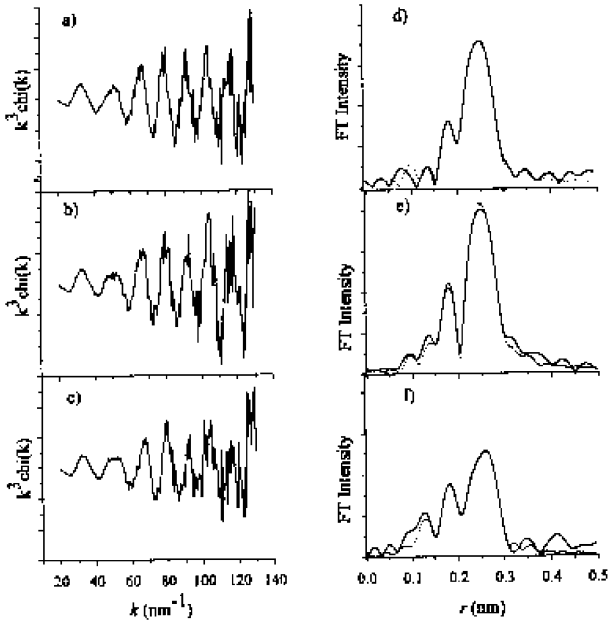

Figure 3. $k^3\chi(k)$-weighted EXAFS oscillation and the Fourier transform in r-space for the PtSn/KL catalyst with a atomic ratio of (a,d) 0.1, (b,e) 0.2 and (c,f) 0.4. The best fitting EXAFS function is plotted as a dotted line in r-space.

Table 2
Structural parameters obtained from EXAFS curve fit for the PtSn/KL catalysts

Sn/Pt	Pair	CN[a]	R (nm)[b]	σ^2 (pm^2)[c]
0.0[d]	Pt–Pt	3.3	0.258	79
	Pt–O	3.5	0.256	584
0.0[e]	Pt–Pt	4.4	0.272	69
	Pt–O	0.2	0.279	−20
0.1	Pt–Pt	4.9	0.272	80
	Pt–Sn	0.3	0.279	77
0.2	Pt–Pt	4.7	0.268	70
	Pt–Sn	0.5	0.280	28
0.4	Pt–Pt	4.5	0.272	93
	Pt–Sn	0.2	0.305	58
	Pt–Sn	0.2	0.195	40

[a]Coordination number (±0.5).
[b]Bond distance (±0.001 nm).
[c]The Debye–Waller factor.
[d]Sample in He with curve fitting with Pt–Pt ad Pt–O shells and taken from the Ref. [8].
[e]Sample in H_2 with curve fitting with Pt–Pt and Pt–O shells and taken from the Ref. [8].

was a substantial change of the chemical state of the Sn. The results of XAFS experiment suggested that the incorporation of Sn into Pt nanoparticles could not cause an increase of particle size, in agreement with the results of xenon adsorption.

The chemical state of Sn in the PtSn/KL catalyst seems to be Sn^{2+} referred from the obtained Pt–Sn distance, which was consistent with the results of Caballero *et al.* [15] and Meitzner *et al.* [16]. Sn contribution to XAFS was

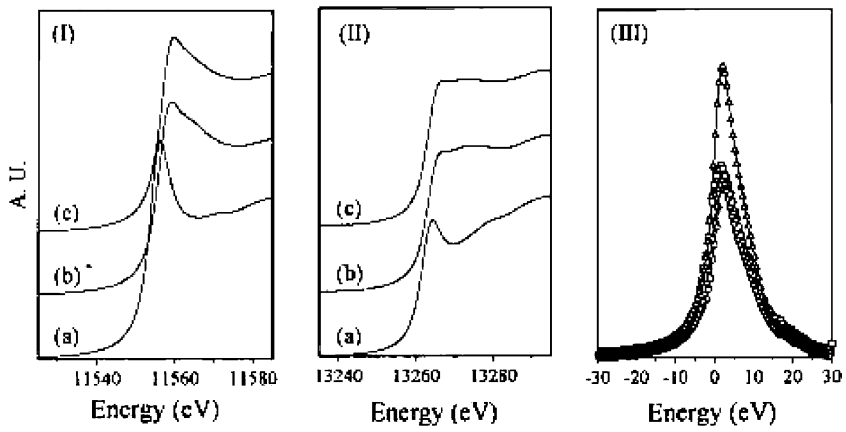

Figure 4. The near edge spectra of (a) the Pt/KL under He, (b) under H_2 gas and (c) the PtSn/KL with an atomic ratio of 0.4 at (I) the Pt L_{III} and (II) Pt L_{II} edges. The obtained difference spectra from the XANES spectra are shown in (III): 2 wt% Pt/KL under He (Δ), 2 wt% Pt/KL under H_2 (O), the SnPt/KL with an atomic ratio of 0.2 (□), and the PtSn/KL with an atomic ratio of 0.4 (∇).

also observed at 0.195 nm, which can be attributed to probably the presence of Sn^{4+} for the SnPt/KL catalyst. The presence of Sn^{4+} may be due to the low reduction temperature, 573 K. Such a high temperature reduction, 773 K, however can cause the loss of active sites for aromatization due to the pore blockage with the growth of the Pt nanoparticles.

Figure 4(I) and (II) show XANES spectra for the PtSn/KL catalysts at the Pt L_{III} and L_{II} edges. It was found that the XANES feature of the PtSn/KL catalysts under He gas was resembled much to that of the Pt/KL catalyst under H_2 gas. Qualitatively, the results suggested that the incorporated tin affects the electronic structure of Pt in a similar manner to hydrogen does. More quantitative information on the electronic structure of platinum can be available from the analysis of the near edge spectra above the Pt L_{III} and Pt L_{II} edges as proposed by Brown *et al.* [17] and Moraweck *et al.* [18]. The hole density in $5d_{5/2}$ can be measured from the difference of the XANES at the Pt L_{III} and L_{II} edges, since the transitions allowed at the Pt L_{III} edge are $2p_{3/2} \rightarrow 5d_{3/2}$ and $5d_{5/2}$ while the transition at the Pt L_{II} edge is $2p_{1/2} \rightarrow 5d_{3/2}$. Therefore, the hole density in $5d_{5/2}$ states is proportional to the difference area $A_{III} - kA_{II}$, where A is area under the XANES peak and k is a constant considering the transition probability.

The difference area of the XANES for the PtSn/KL catalysts is shown in figure 4(III). The obtained difference area of the XANES for the PtSn/KL catalysts was the same as that of the Pt/KL catalyst with adsorbed hydrogen. The results of the XANES analysis suggested that electron transfer occurred from Sn to Pt, which was agreed with those of PtSn bimetallic nanoparticles supported on γ-Al_2O_3 by Caballero *et al.* [15] and Davis [19]. Thus, it seems that the incorporation of tin into Pt nanoparticles consisting of 5–7 atoms cause a significant change in the *d* band structure as much as hydrogen adsorption does.

n-Hexane aromatization over the PtSn/KL catalysts was performed at 671 K with $H_2/C_6H_{14} = 6$. Turnover frequency (υ_t) based on the amount of total Pt decreased progressively with the increase of Sn content near 10% conversion level of *n*-hexane aromatization as shown in figure 5. The decrease of catalytic activity for *n*-hexane aromatization seems probably due to the surface coverage of Sn over Pt nanoparticles in the PtSn/KL catalyst. The product distribution of *n*-hexane aromatization is also illustrated in figure 6. The reaction data were consistent with that the incorporation of Sn onto the Pt nanoparticles suppress an isomerization

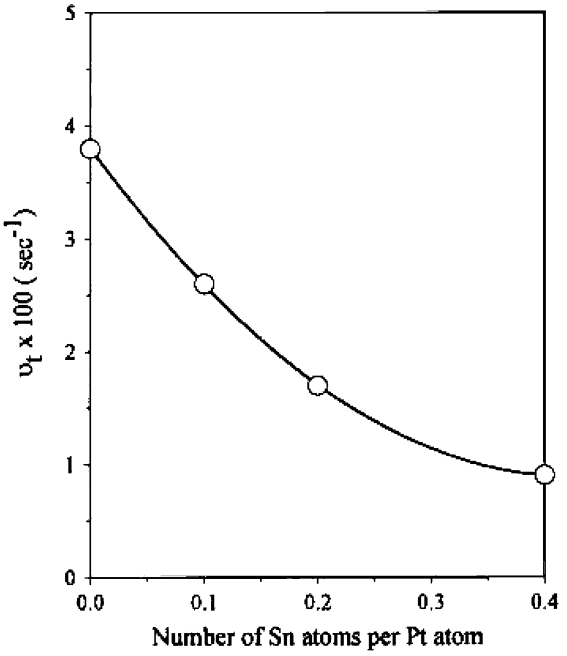

Figure 5. The catalytic activity of *n*-hexane aromatization over the PtSn/KL catalysts plotted against the atomic ratio of Sn/Pt. The reaction was performed at 671 ± 1 K with $H_2/C_6H_{14} = 6$. υ_t was based on the total amount of Pt.

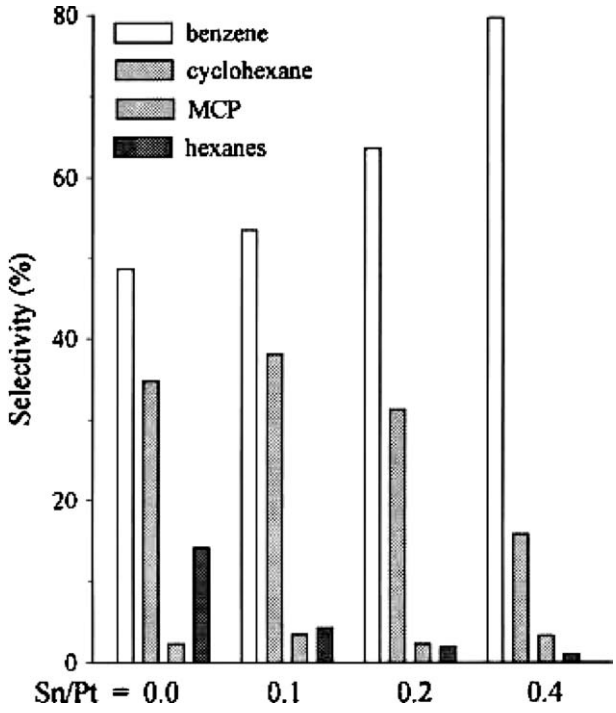

Figure 6. The product selectivity of *n*-hexane aromatization over the PtSn/KL catalysts is illustrated with increasing the Sn/Pt ratio at near 10% conversion. The selectivity was defined as $C_i/\Sigma C_i \times 100$ where C_i was the number of moles produced.

to hexanes and 1,5-ring formation to methylcyclopentane, resulting in an increased selectivity to benzene from 50% to 80% with the Sn content. The content of potassium in the SnPt/KL catalyst was controlled to 8.49 ~ 8.29 K^+ ion depending on the content of tin. The effect of such a small change of alkali loading in the KL zeolite seems to be negligible under the present reaction condition.

The reaction data under the similar alkali loading, combined with the result of characterization data suggested that the decrease of Pt ensemble size by tin can suppress the formation of highly dehydrogenated species required for hydrogenolysis, isomerization and coke deposition, resulting in the high selectivity to benzene. Also, it was believed that the change of electronic structure of the nanoparticles referred from the result of XANES may affect the adsorption characteristics of reactants such as hydrogen and similarly benzene.

4. Conclusion

Incorporation of tin into the Pt nanoparticles containing 5–7 atoms inside KL zeolite changed significantly the adsorption properties of hydrogen and xenon and the ^{129}Xe NMR chemical shift, which are consistent with the formation of bimetallic nanoparticles. The results of XAFS experiment and xenon adsorption method suggested the formation of the PtSn nanoparticles inside the KL zeolite channel without a pore blockage. Catalytic performance of the PtSn/KL catalyst over n-hexane aromatization can be improved with mainly the Pt ensemble effect by an incorporation of tin. The modified electronic structure of the nanoparticles may affect the hydrogen adsorption.

References

[1] R. Srinivasan and B.H. Davis, Platinum Met. Rev. 36 (1992) 119.
[2] B.C. Gates, Chem. Rev. 95 (1995) 511.
[3] P. Meriaudeau, C. Naccache, A. Thangaraj, C.L. Bianchi, R. Carli, V. Vishvanathan and S. Narayanan, J. Catal. 154 (1995) 345.
[4] C. Xu, Y.L. Tsai and B.E. Koel, J. Phys. Chem. 98 (1994) 585.
[5] R.D. Cortright and J.A. Dumesic, Appl. Catal. A: Gen. 129 (1995) 101.
[6] S.J. Cho, W.S. Ahn, S.B. Hong and R. Ryoo, J. Phys. Chem. 100 (1996) 4996.
[7] R. Ryoo, S.J. Cho, C. Pak and J.Y. Lee, Catal. Lett. 20 (1993) 107.
[8] H. Ihee, T. Becue, R. Ryoo, C. Potvin, J.-M. Manoli and G. Djega-Mariadassou, Stud. Surf. Sci. Catal. 84 (1994) 765.
[9] J.C. Schlatter and M. Boudart, J. Catal. 24 (1974) 482.
[10] R. Ryoo, C. Pak and S.J. Cho, Jpn. J. Appl. Phys. 32; Suppl. 32-2 (1993) 475.
[11] D.H. Ahn, J.S. Lee, M. Nomura, W.M.H. Sachtler, G. Moretti, S.I. Woo and R. Ryoo, J. Catal. 133 (1992) 191.
[12] E.A. Stern, M. Newville, B. Ravel, Y. Yacoby and D. Haskel, Physica B 208 (1995) 117.
[13] M. Newville, P. Livins, Y. Yacoby, J.J. Rehr and E.A. Stern, Phys. Rev. B 47, (1993) 14126.
[14] J.J. Rehr, R.C. Albers and S.I. Zabinsky, Phys. Rev. Lett. 69 (1992) 3397.
[15] A. Caballero, H. Dexpert, B. Didillon, F. LePeltier, O. Clause and J. Lynch, J. Phys. Chem. 97 (1993) 11283.
[16] G. Meitzner, G.H. Via, F.W. Lytle, S.C. Fung and J. H. Sinfelt, J. Phys. Chem. 92 (1988) 2925.
[17] M. Brown, R.E. Peierls and E.A. Stern, Phys. Rev. B 15 (1977) 738.
[18] B. Moraweck, A.J. Renouprez, E.K. Hlil and R. Baudoing-Savois, J. Phys. Chem. 97 (1993) 4288.
[19] B. H. Davis, Stud. Surf. Sci. Catal. 75 (1992) 799.